

Gasdynamic effects of a ring surface discharge

N. K. Berezhetskaya, E. F. Bol'shakov, S. K. Golubev, A. A. Dorofeyuk, I. A. Kosyĭ, V. E. Semenov, and V. E. Terekhin

Institute of General Physics, Academy of Sciences of the USSR, Moscow

(Submitted 21 June 1984)

Zh. Eksp. Teor. Fiz. **87**, 1926–1931 (December 1984)

Shadow photography and a piezoelectric transducer were used in a study of the gasdynamic effects of a ring surface discharge. It was found that cumulative shock waves formed in such a discharge. The main characteristics of these waves in a ring system were similar to the characteristics of a cylindrical cumulative shock wave.

An experimental investigation was made of the gasdynamic effects of a ring surface discharge set up in accordance with a scheme described in Ref. 1. A cable was formed into a ring and then ring electrodes separated by a gap of about 0.5 cm were placed on the surface of an insulator from which the screening braid was removed. The central core of the cable was connected to the last electrode located at the end of the cable. The construction of the discharge ring and the electrical circuit are shown schematically (Fig. 1). Short-circuiting of a discharge gap DG released the energy stored in a capacitor C and this energy was used to initiate and maintain surface "creep" discharges between the electrode. Short-circuiting of the discharge gap caused the charging voltage U of the capacitor to be applied to the first gap between the electrodes (i.e., to the gap closest to the part of the cable on which the braid was retained). This resulted in a sequence of breakdowns which spread over the whole multielectrode ring-shaped region in a time of less than $0.5 \mu\text{sec}$. The current through the discharge ring was a damped sinusoid with a period of the order of $10 \mu\text{sec}$. The total discharge time depended on the pressure in the gaseous medium and amounted to $t_d = 25\text{--}50 \mu\text{sec}$.

The radius of the ring was $r = 50 \text{ mm}$ and its width was $\Delta = 10 \text{ mm}$. The energy stored in the capacitor was $W \leq 100 \text{ J}$. The ring was inside a chamber filled with nitrogen, air, or argon at a pressure in the range $1 \leq p \leq 760 \text{ Torr}$.

The method of shadow photography with a laser light source² was used to record gasdynamic perturbations created by the ring discharge. This was done for two orientations of the ring: with the plane of the ring orthogonal ($S \perp z$) and parallel ($S \parallel z$) to the axis of a diagnostic beam. A characteris-

tic time sequence of shadowgrams obtained in the orthogonal case is shown in Fig. 2 ($p_0 = 300 \text{ Torr}$, $U = 18 \text{ kV}$). The time intervals between the frames were known, but the first frame of the shadowgram was not recorded exactly at the moment of triggering of the ring discharge. Assuming that the first shadow image corresponded to the moment in time within $t_1 \approx 0\text{--}25 \mu\text{sec}$ from the beginning of the ring surface breakdown, we found that the subsequent frames corresponded to time delays $t_2 \approx 75\text{--}100 \mu\text{sec}$, $t_3 \approx 125\text{--}150 \mu\text{sec}$, $t_4 \approx 150\text{--}175 \mu\text{sec}$, and $t_5 \approx 175\text{--}200 \mu\text{sec}$. The duration of the laser radiation pulse used in shadow photography was $\tau_l \approx 20 \text{ nsec}$.

An analysis of the shadowgrams yielded the following conclusions.

a) Each of the discharge gaps located on the ring surface became a source of shock waves (frame 1 in Fig. 2). The gasdynamic perturbations interacted with one another and produced a ring shock wave in the plane of the ring discharge and this wave converged at the center of the ring. Outside the plane of the ring discharge the elementary gasdynamic perturbations "crossed" each other without interaction.

b) In approximately $75 \mu\text{sec}$ from the formation of the first ring shock wave it was found that a second converging wave formed in the ring discharge plane (frame 2 in Fig. 2).

c) The first ring wave collapsed (frame 3 in Fig. 2) and after reflection at the center (frame 4 in Fig. 2) traveled to the periphery and at some distance from the latter encountered the second ring shock wave (frame 5 in Fig. 2).

The fact that the elementary shock waves were visible only in the lower part of frame 1 in Fig. 2 was the result of a tilt of the diagnostic laser beam relative to the ring axis. The departure from the azimuthal symmetry of the ring shock wave (manifested by a characteristic "loop" in the upper left-hand side of frame 2 in Fig. 2) appeared at the point of discontinuity in the discharge ring (where the leads were located). A constant background in the shadowgrams manifested by concentric rings filling the optical field with rigorously kept periods was a methodological shortcoming associated with the selected optical system employed in our measurements. The velocity of the first ring shock wave before the onset of collapse (at sufficient distance from the axis) was deduced from the shadowgrams and found to be about $6 \times 10^4 \text{ cm/sec}$ ($2M$), but after reflection from the center it rose to about $9 \times 10^4 \text{ cm/sec}$ ($3M$); these values were ob-

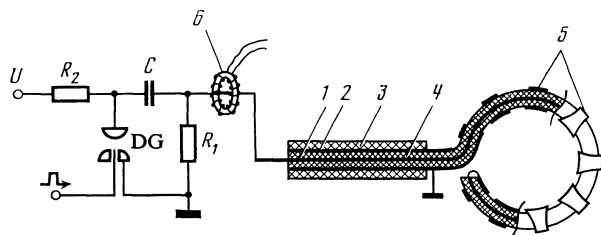


FIG. 1. Electrical circuit and construction of the discharge ring: 1) high-voltage core of a cable; 2) screening braid; 3) outer insulator; 4) inner insulator; 5) ring electrodes; 6) Rogowski loop.

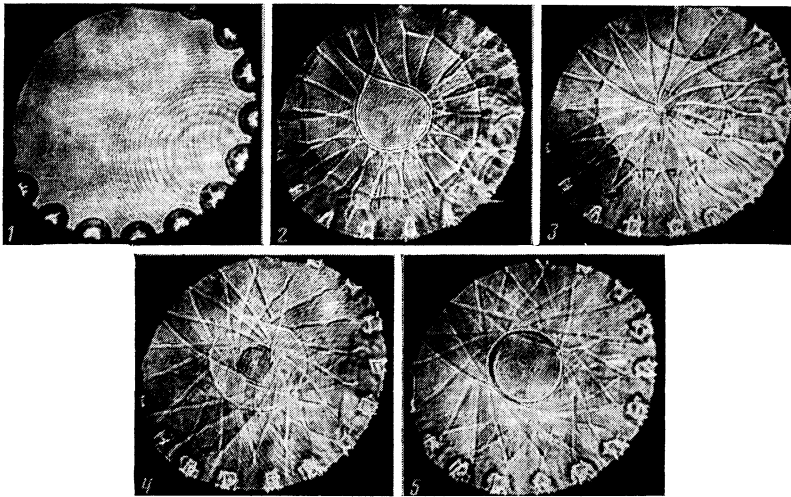


FIG. 2. Shadowgrams of the region inside the ring ($p_0 = 300$ Torr, $U = 18$ kV: 1) $t \approx 0-25$ μ sec; 2) $t \approx 75-100$ μ sec; 3) $t \approx 125-150$ μ sec; 4) $t \approx 150-175$ μ sec; 5) $t \approx 175-200$ μ sec.

tained at a pressure $p_0 = 300$ Torr.

Shadow photography in the form used in the present study allowed us to establish only the fact of appearance of a shock wave, but it did not provide spatial resolution sufficient for the determination of the actual width of a density discontinuity in the shock wave front.

The results of an investigation of the structure of the gasdynamic perturbations by shadow photography were supplemented by measurements of the pressure discontinuity near the axis carried out using a piezoelectric transducer. A piezoelectric crystal was placed outside the ring and was connected acoustically to the axial region of the ring by an acoustic guide in the form of a ceramic cylinder 4 mm in diameter. A special system made it possible to displace the transducer and the acoustic guide in the radial direction. A typical oscillogram of the transducer signal is shown in Fig. 3. The arrow identifies the moment of the onset of the ring surface discharge. The first positive pulse after triggering of the discharge represented a stray signal induced in the recording apparatus. The transducer signal appeared after a time delay of $\tau \approx 100-120$ μ sec, which represented the transit time of the first cylindrical shock wave traveling from the ring to the acoustic guide surface and of the acoustic wave

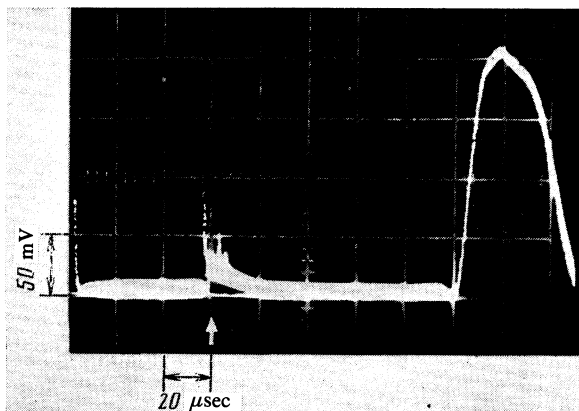


FIG. 3. Typical oscillogram of a signal produced by the piezoelectric transducer.

traveling from the end of the acoustic guide to the surface of the transducer.

The dependence of the pressure discontinuity on the ring axis on the initial pressure in the chamber was determined on the basis of oscillograms similar to that shown in Fig. 3: it was a function that increased monotonically on reduction in p_0 . For the maximum input energy delivered to the surface discharge ($W \approx 100$ J) the ratio of the pressure p behind the front of the first converging ring shock wave to the original pressure p_0 in the chamber was $p/p_0 \approx 50$ for $p_0 = 75$ Torr and $p/p_0 \approx 10$ for $p_0 = 760$ Torr.

The change in the pressure behind the front of the ring shock wave on approach to the axis is illustrated in Fig. 4. It is clear from this figure that the ratio $p/p_0 = f(r)$ (with the value r measured from the axis of the ring) first fell slowly and then began to rise on approach to the axis. An analysis of dependences similar to that shown in Fig. 4 indicated that during the cumulation process the pressure in the shock

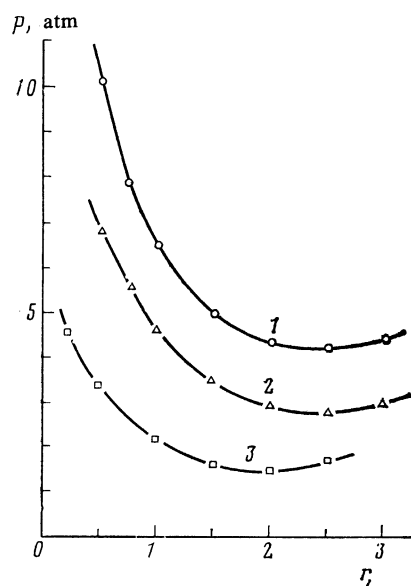


FIG. 4. Variation of the amplitude of a shock wave on approach to the center of the ring: 1) $p_0 = 750$ Torr; 2) $p_0 = 300$ Torr; 3) $p_0 = 75$ Torr.

wave converging at the center of the ring obeyed the relationship

$$p(r) = Ar^{-n}, \quad (1)$$

where A depended on the initial pressure and the nature of the gas and the power exponent was $n = 0.6 \pm 0.2$.

Both shadow photography and the piezoelectric transducer measurements indicated cumulation of the shock wave created by the surface discharge. Such enhancement of the ring wave was not a trivial effect because, in contrast to a converging spherical or cylindrical shock wave, in the ring geometries the energy could be carried away out of the cumulation region in the axial direction. The nonlinear problem of the case of a ring shock wave cannot be solved analytically. Qualitative estimates obtained by dimensional analysis and on the basis of the law of conservation of energy are very fruitful when diverging shock waves created by an instantaneous explosion are analyzed, but they fail to give the main characteristics of cumulation of a ring shock wave because in the cumulation process the leading edge of a shock wave "runs away" from the bulk of the energy deposited in the gas and no energy is generally evolved in the focusing region.³ Therefore, various simplified models have to be used to investigate the feasibility and nature of cumulation of a ring shock wave.

In particular, the possibility that, in principle, a gasdynamic perturbation may be amplified can be studied employing a linear model describing the evolution of weak acoustic waves:

$$\partial^2 p / \partial t^2 - c^2 \Delta p = (\gamma - 1) \partial q / \partial t, \quad (2)$$

where p is the excess pressure; c is the velocity of sound; γ is the adiabatic exponent of gaseous medium; q is the power density of the heat source which excites the investigated sound. First of all, we must point out that a solution of Eq. (2) subject to zero initial conditions is

$$p(\mathbf{r}, t) = \frac{\gamma - 1}{4\pi c^2} \int \frac{1}{|\mathbf{r} - \mathbf{r}'|} \frac{\partial}{\partial t} q\left(\mathbf{r}', t - \frac{|\mathbf{r} - \mathbf{r}'|}{c}\right) d^3 \mathbf{r}' \quad (3)$$

and it shows that for any source without singularities (when $\partial q / \partial t$ is finite) the acoustic signal is always and everywhere finite. The unbounded cumulation of spherical and cylindrical converging shock waves considered in the acoustic approximation⁴ applies only when a wave has an absolutely abrupt leading edge (i.e., when the source is activated instantaneously). Saturation of the cumulation process is related to reflection of the incident wave from the center of symmetry and is characteristic of any system of acoustic waves with a nonabrupt leading edge.

The dependence of enhancement of a wave at the center on the steepness of its leading edge can be illustrated by considering a general solution for a spherically symmetric acoustic wave:

$$p(r, t) = r^{-1} \{f(ct+r) - f(ct-r)\}, \quad p(0, t) = 2f'(ct), \quad (4)$$

where $f(\xi)$ is an arbitrary function and $f'(\xi)$ is its first derivative.

The main characteristics of the evolution of a ring

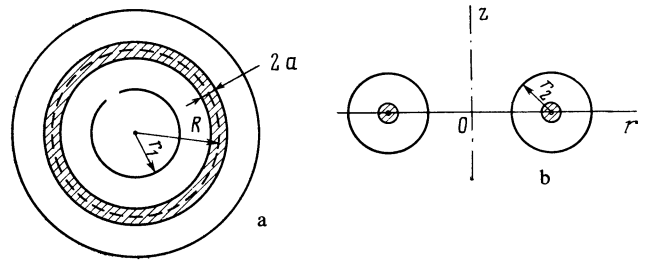


FIG. 5. Ring heat source (shown shaded) and the front of a ring wave: a) principal plane; b) plane passing through the symmetry axis z .

acoustic wave can be investigated by selecting a heat source concentrated inside a toroidal ring with radii a and R ($a \ll R$, see Fig. 5). An analysis of the general expression (4) shows that the maximum excess pressure in the front of a ring wave in the main plane of the torus can be estimated from

$$p_{\max}(r) = p_{\max}(R) \left[\frac{aR}{(R-r)r} \right]^{1/2} \quad (5)$$

Here, r is the distance from the leading edge of the wave to the center of symmetry and $p_{\max}(R)$ is the maximum excess pressure in the region of the source. According to Eq. (5), the pressure in the front of a ring wave first begins to decrease (as in a diverging cylindrical wave), but on approach to the center of symmetry it rises as in a converging cylindrical wave. It follows from the above that enhancement of the amplitude of a ring wave is limited to distances from the center of the order of the thickness A of the leading edge of the front and the maximum excess pressure is

$$p_{\max}(0) = p_{\max}(R) (a/\Lambda)^{1/2}. \quad (6)$$

Therefore, cumulation of a ring wave is, in principle, possible. However, under the experimental conditions described above the thickness of the leading edge of an acoustic wave was of the order of the thickness of the ring source ($a \sim \Lambda$), so that in the acoustic approximation we can assume that $p_{\max}(0) \sim p_{\max}(R)$.

Evolution of a high-intensity acoustic wave generally results in the formation of a shock wave. This is primarily manifested by steepening of the leading edge and, as we have seen above, it tends to enhance cumulation. On the other hand, the velocity of a shock wave depends on its amplitude. This may result in distortion of the shape of the leading edge. Cumulation of a ring acoustic wave at the center of symmetry is of the same nature as in the case of a converging cylindrical wave. This is due to the fact that near the center the radius of curvature r_1 of the leading edge in the principal plane of the torus is much less than the radius of curvature r_r in a plane perpendicular to the torus plane (Fig. 5). If this is also true of a ring shock wave, then obviously the cumulation will be also analogous to the cumulation of cylindrical shock wave. Possible distortions of the front of a ring shock wave in the vicinity of the center of symmetry may be analyzed on the basis of the following simple considerations. If $r_1 \ll r_2$, then in each plane $z = \text{const}$ near the principal one ($z = 0$) the motion of the shock wave front can be considered analogously to the motion of the front of a converging cylindrical wave at a given distance from the axis:

$$\partial r / \partial t = A r^{-(1-\alpha)/\alpha}, \quad (7)$$

where A is governed by the power of the source and α is the power exponent of the self-similar solution for a cylindrical wave.⁴ A simple calculation shows that although $r_2 \rightarrow 0$ in the limit $r_1 \rightarrow 0$, the ratio r_2/r_1 rises without limit. Consequently, the main characteristics of the cumulation of a ring shock wave are identical to those encountered in the cumulation of a cylindrical wave, i.e., for $r \ll R$ the distance rises in accordance with the law (if $\gamma = 7/5$)

$$p(r) \propto r^{-0.395}. \quad (8)$$

We should point out also the experimental observation of a second converging shock wave which appeared after a time interval $t \approx 75 \mu\text{sec}$ greater than the duration of the existence of the surface discharge. The origin of the second ring shock wave is not clear. We may assume that it is associated with electron recombination in a cooling plasma.

The variant of a ring source of a shock wave described in our study may be useful in laboratory practice as a relatively simple device that can generate large discontinuities of the

pressure, temperature, and density of the gaseous medium at the point of collapse.

The authors are grateful to G. M. Batanov, V. S. Imshennik, L. M. Kovrizhnykh, and A. A. Rukhadze for discussions and valuable comments.

¹N. K. Berezhetskaya, E. F. Bal'shakov, A. A. Dorofeyuk, *et al.*, Preprint No. 244 [in Russian], Lebedev Physics Institute, Academy of Sciences of the USSR, Moscow, 1983.

²L. A. Dushin and O. S. Pavlichenko, *Issledovanie plazmy s pomoshch'yu lazerov* (Investigation of Plasmas by Lasers), Atomizdat, M., 1968.

³Ya. B. Zel'dovich and Yu. P. Raizer, *Fizika udarnykh voln i vysokotemperaturnykh gidrodinamicheskikh yavlenii*, Nauka, M., 1966, p. 610 (Physics of Shock Waves and High Temperature Hydrodynamic Phenomena, 2 vols., Academic Press, New York, 1966, 1967).

⁴E. I. Zababakhin, *V sb.: Mekhanika v SSSR za 50 let* (in: Mechanics in the USSR During Last 50 Years), Vol. 2, Nauka, M., 1970, p. 313.

Translated by A. Tybulewicz